5-2016

Shrinkage Analysis of Carbon Micro Structures Derived from SU-8 Photoresist

Rucha Natu
Clemson University

Monsur Islam
Clemson University

Rodrigo Martinez-Duarte
Clemson University, rodrigm@clemson.edu

Shrinkage Analysis of Carbon Micro Structures Derived from SU-8 Photoresist

R. Natu, M. Islam and R. Martinez-Duarte
Department of Mechanical Engineering, Clemson University, Clemson, South Carolina 29634, USA

Abstract

We present preliminary results for the analysis of shrinkage of 3D carbon posts obtained by the pyrolysis of SU-8 precursor structures, in a technique known as Carbon MEMS. Though the shrinkage in the carbon structures is highly reproducible, there is a strong dependence of this shrinkage on the initial dimensions of the SU-8 pillars. Our hypothesis is that the shrinkage depends upon the area available for degassing during carbonization. In this work, this idea is used to analyze shrinkage in cylindrical pillars. The results obtained are studied based on the ratio of lateral and top surface area available for degassing and reinforce the hypothesis about the dependence on surface area.

Introduction

SU-8 is a negative photoresist featuring high-transparency in the UV range. This characteristic allows for its use in the fabrication of thick and/or high aspect ratio structures for applications that include molds for soft lithography (1) and structural elements in microfluidics (2). Of particular interest here is the use of SU-8 photolithography to fabricate structures that are then carbonized following a technique known as Carbon MEMS. The pyrolysis of SU-8 structures at high temperatures under inert atmosphere yields glass-like carbon features that have been used to implement batteries (3), fuel cells (4), sensors (5), and bio particle filters (6-11).

Shrinkage occurs during the carbonization of SU-8 structures but the geometry of the precursor is preserved. This is due to the fact that the temperature ramp during the process is controlled so the temperature in the oven is always lower than the glass transition temperature of the material at any given temperature (photoresist/carbon). Previous reports showed a near isometric shrinkage of the precursor structure during carbonization (11). Although this shrinkage is highly reproducible for a given structure and carbonization protocol, there seems to be a strong dependence of shrinkage on the initial dimensions of the SU-8 pillars. Shrinkage can be as low as 30% when pyrolyzing tall and slender features and increase to 90% when carbonizing thin films (11, 12).

In this work we aim at elucidating the mechanisms that determine the percentage of shrinkage when carbonizing SU-8 structures. The goal is to obtain a model that can successfully predict the amount of shrinkage for a SU-8 structure of given dimensions. This will prove useful in the design stage of a number of devices to be used in the applications mentioned above. For example, in the fabrication of carbon post electrodes for bio particle filtering and manipulation using electric field gradients.

Materials and Methods

SU-8 (Gersteltec, Switzerland) structures were fabricated on a silicon substrate using photolithography. The fabrication parameters for cylindrical posts were optimized (data not shown) to yield the values shown in Table 1. Cylindrical posts with height of 10, 50 and 100 µm and diameters of 10, 20, 30, 40, 60 and 80 µm were attempted to be fabricated. The aspect ratio, height *h*/Diameter *D*, of the designed *versus* fabricated structures is shown in Figure 1. All calculations regarding shrinkage were made using the dimensions of the fabricated cylinders.

TABLE I. Fabrication details for cylindrical posts

Height of Post (µm)	Type of SU-8	Spin Coating			Soft Bake at 95 °C (min)	Exposure (mJ/cm^2)	PEB at 95 °C (min)	Develop in PGMEA (min)
		Step	Speed (rpm)	Time (s)				
10	GM 1060	1	500	10	30	225	20	3
		2	2500	40				
50	GM 1075	1	500	10	60	165	60	6
		2	3000	100				
100	GM 1075	1	500	10	60	210	60	8
		2	1700	100				

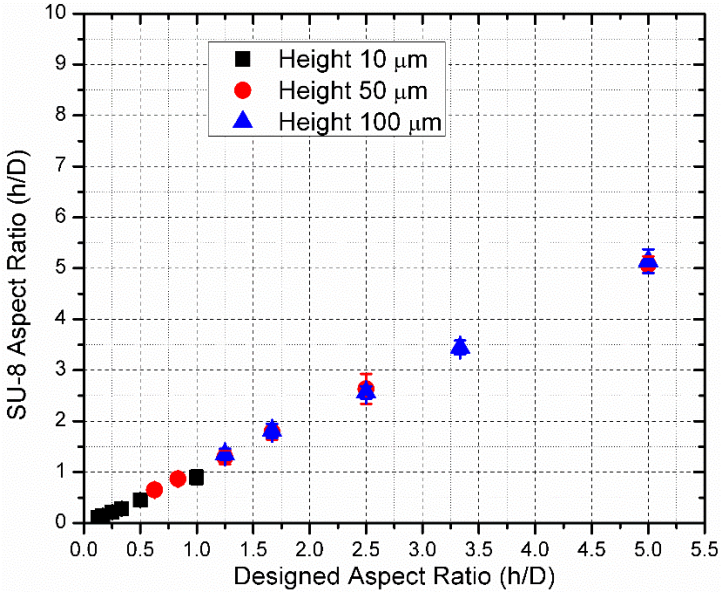

Figure 1. Aspect ratio of designed post vs. aspect ratio of fabricated SU-8 post. The vast majority of the fabricated posts were true to the designed dimensions.

The structures were pyrolyzed in vacuum or nitrogen atmosphere at the temperatures of 600, 900, 1150 and 1300˚C in a tube furnace (TF1700, Across International) using a two-step process where a dwell of 30 minutes is introduced at 300 °C before ramping up to the final temperature. The average values of height *h* and diameter *D* of the SU-8 posts and the product after pyrolysis were determined using a surface profiler (Tencor Alpha Step 200) and an optical microscope (Nikon Eclipse LV100) respectively. These measurements allowed for the calculation of surface area ($\pi Dh+\pi D^2/4$), volume ($\pi D^2 h/4$), and aspect ratio (h/D) for all cylinders before and after pyrolysis. The percentage shrinkage was calculated using equation 1, where the dimension can take the form of height or diameter as specified in each case below.

$$\%\, Shrinkage = \frac{Initial\ Dimension - Final\ Dimension}{Initial\ Diemsion} * 100 \qquad [1]$$

Results and Discussion

The structures obtained after pyrolysis retained their original shape but showed considerable shrinkage. Results are shown in figure 2. Similar to results obtained by other authors (13), it was observed that the shrinkage in height for tall posts is less than that seen with shorter posts of the same cross section. In order to analyze shrinkage, the % shrinkage in height and diameter, as calculated using equation 1, was plotted against the aspect ratio of the original SU-8 post (fig. 2A). The shrinkage in diameter goes on increasing with the aspect ratio and finally approaches a constant value of around 45-50% at aspect ratios beyond 5. In contrast, the shrinkage in height is most at low aspect ratios and decreases as the aspect ratio increases. The shrinkage in height stabilizes around 50%, also at aspect ratios beyond 5. The same data was then plotted against the total surface area of the different SU-8 features. For a cylinder, the surface area considered here will be its walls and only its top, as the bottom of the cylinder is the face making contact with the substrate. The results are plotted in figure 2B. In this case the shrinkage in diameter goes on decreasing with an increase on surface area. This change is very evident especially in the case of structures with height 10 µm. These results suggest that an increase of surface area leads to decrease in diametrical shrinkage when the structures are short. The change of shrinkage is considerably less for features with the same surface area but higher thickness. In other words, short and wide features seem to show different trend in shrinkage than the tall, slender ones even when they both have the same surface area. Hence, by comparing figures 2A and B, it became clear that the distribution of surface area, not just the total surface area, is the important parameter to consider. The next step was then to plot the lateral surface area over the surface area of the top of the cylinder. Results are shown in figure 2C. As this ratio goes beyond 5, the shrinkage reaches a stable value around 50%. To validate the shrinkage values obtained, the shrinkage for the posts reported by Amato *et. al.* are also plotted in Figure 2C (14). Even though the diameters of their cylinders was as small as 1 µm, but still featuring aspect ratios of 10, it can still be seen that these values fall in the range of the values obtained in this work.

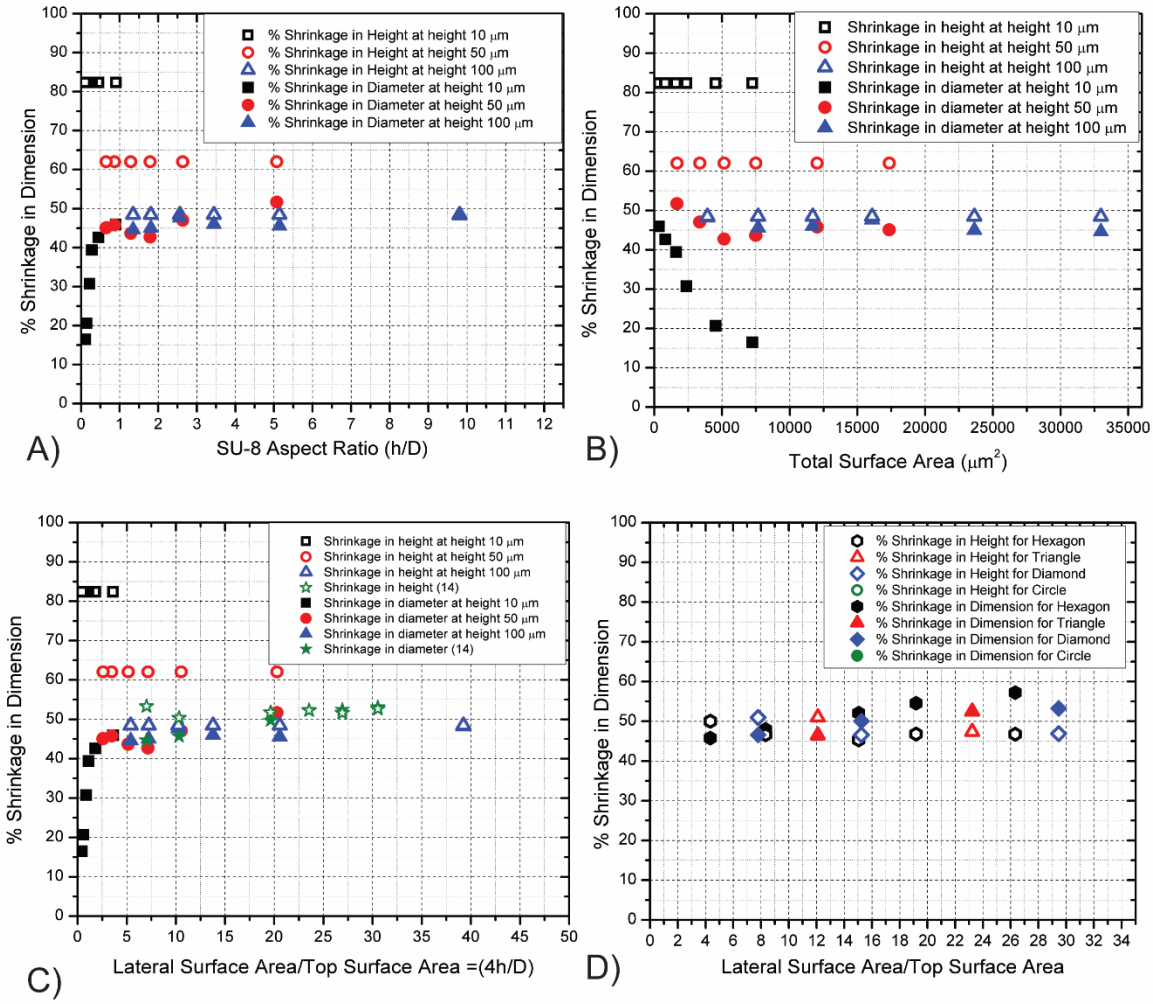

Figure 2. A) Percent shrinkage in Radius and Height with respect to aspect ratio of the cylindrical posts. B) Percent shrinkage in radius and height with respect to the total surface area of the post. C) Percent shrinkage in radius and height with respect to the ratio of lateral and top surface areas. The plot also shows the data points for reference (14). D) The plot shows the percent shrinkage in characteristic dimension for different shapes with respect to the ratio of lateral to top surface area. (Error bars are omitted here because they are the same magnitude as that of the symbols shown in the plot). All plots are for the data at 900°C in nitrogen atmosphere.

Carbonization is a complex process with dehydrogenation, condensation, hydrogen transfer and isomerization occurring concurrently. During pre-carbonization, which takes place below the temperature of 300°C, molecules of solvent and unreacted monomer are eliminated from the polymeric precursor. In the next step, carbonization, from 300 to 500 °C, oxygen is eliminated, causing a rapid loss of mass, while a network of conjugated carbon systems is formed and hydrogen atoms start being eliminated. During the third stage, up to the temperature of 1200°C, hydrogen, oxygen and nitrogen atoms are completely eliminated and the aromatic network is forced to become interconnected. The final pyrolysis temperature determines the degree of carbonization and the residual content of foreign elements. At final temperatures above 900 °C, the carbon content of the residue is expected to exceed a mass fraction of 90% in weight (11).

Shrinkage occurs as the SU-8 gets carbonized and the products of this process escape as gasses, leaving behind a solid carbon structure. Thus, the shrinkage phenomenon is related to the degasification of SU-8. The distribution of lateral over top surface area is important in an attempt to predict shrinkage. When the gasses escape from the top surface area, they result in the shrinkage of the height of the post; when they escape from the lateral surface area, lateral shrinkage occurs. As the diameter of the post increases, the gasses trapped at the core find it difficult to escape from the lateral regions, resulting in less lateral shrinkage. On the other hand, lateral shrinkage is more pronounced when the post is tall and slender. Thus, whenever the lateral surface area dominates, the shrinkage is more along the lateral dimensions and when the top surface area dominates in the total surface area, height shrinkage is the dominant phenomena.

In order to validate this observation, the percent shrinkage for high aspect ratio (>5) structures with different cross sectional shapes was obtained and plotted against the ratio of the lateral to top surface area of the corresponding shapes. The shrinkage in these cases is very similar to that of the cylindrical structures previously obtained. Since the ratio value is higher than 5, the lateral area available for degassing always dominates.

Another parameter of study was the effect of the atmosphere in the tube furnace during pyrolysis. The shrinkage of the structures when pyrolyzed in nitrogen and vacuum is presented in figure 3. Although shrinkage seems to be lower in the case of a nitrogen atmosphere, the difference is minimal and further studies are needed to draw a valid conclusion. The hypothesis is that the degree of degassing during carbonization depends on the pressure difference between the structure core and the environment (15). We believe that degassing and diffusion of gaseous byproducts are increased when using vacuum since a negative pressure gradient is established. In the nitrogen atmosphere, positive pressure gradient acts on the structure to slow down the process of diffusion. Hence, higher shrinkage is expected when using vacuum conditions.

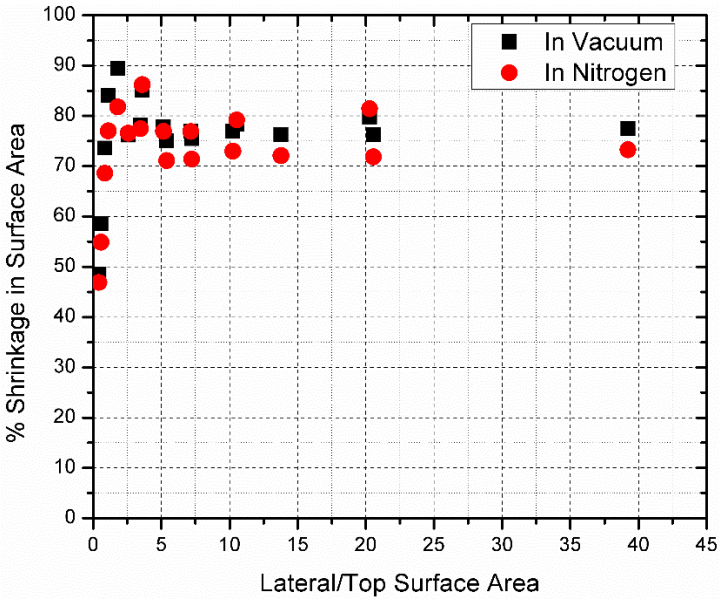

Figure 3. Percent shrinkage in surface area when using vacuum or nitrogen atmospheres for pyrolysis at 900 °C. A clear difference between both atmospheres cannot be discerned.

Conclusion and Future work

In this work the shrinkage behavior of different sizes of SU-8 3D carbon posts was studied. Cylindrical posts with different heights and varying cross sectional areas were examined to find a relationship between shrinkage and geometry of the post. Shrinkage depends on degassing of the pyrolysis byproducts during the process. Degassing occurs through the surface area of the structure, thus shrinkage in a particular dimension, *i.e.* the height or the diameter of the posts, depends on the surface area of such dimension. Since the shrinkage a particular structure seems to depend on the geometrical surface area available for degassing, this can be used as a design guideline in attempt to predict shrinkage.

The relation of the shrinkage with the ratio of the lateral to top surface area was obtained. Importantly, the shrinkage in the characteristic length of the shape increases with an increase in this ratio, whereas the shrinkage in height decreases with an increase in such ratio. The value of shrinkage reaches a stable value of around 50% when the lateral surface area is almost five times the top surface area. This behavior of obtaining a stable shrinkage for ratios higher than 5 was validated using different cross sections for the posts. A mathematical model for shrinkage depending on this ratio constitutes the future task in this work. Different cross sectional posts with a ratio less than 5 should also be studied to obtain the results and see if the behavior is similar to the one shown by cylindrical posts.

Based on the results obtained for the nitrogen atmosphere and vacuum, it can be seen that along with the surface area, the pyrolysis atmosphere may play an important role in the amount of shrinkage. Ongoing work is on studying this relationship to develop a more concrete model for shrinkage.

Acknowledgments

The authors would like to thank Emanuele Giolgi for kindly providing measurements of different SU-8 and carbon structures.

References

1. P. Abgrall, V. Conedera, H. Camon, A. M. Gue, and N. T. Nguyen, *Electrophoresis*, **28**, 4539 (2007).
2. R. Martinez-duarte and M. J. Madou, in *Microfluidics and Nanofluidics Handbook: Fabrication, Implementation and Application*, S. Chakraborty and S. Mitra, Editors, p. 231–268, CRC Press (2011).
3. C. Wang et al., *Electrochem. Solid-State Lett.*, **7**, A435 (2004).
4. B. Y. Park and M. J. Madou, *J. Power Sources*, **162**, 369 (2006).
5. H. Xu et al., *Biosens. Bioelectron.*, **23**, 1637 (2008).
6. M. D. C. Jaramillo et al., *Biosens. Bioelectron.*, **43**, 297 (2013).
7. M. D. C. Jaramillo, E. Torrents, R. Martínez-Duarte, M. J. Madou, and A. Juárez, *Electrophoresis*, **31**, 2921 (2010).
8. R. Martinez-Duarte, PhD Mechanical and Aerospace Engineering, University of California, Irvine (2010).
9. R. Martinez-Duarte, *Electrophoresis*, **33**, 3110 (2012).

10. R. Martinez-Duarte, F. Camacho-Alanis, P. Renaud, and A. Ros, *Electrophoresis*, **34**, 1113 (2013).
11. R. Martinez-Duarte, P. Renaud, and M. J. Madou, *Electrophoresis*, **32**, 2385 (2011).
12. B. Y. Park, L. Taherabadi, C. Wang, J. Zoval, and M. J. Madou, *J. Electrochem. Soc.*, **152**, J136 (2005).
13. R. Martinez-Duarte, *Micromachines*, **5**, 766 (2014).
14. L. Amato et al., *Carbon N. Y.*, **94**, 792 (2015).
15. L. A. Liew et al., *Sensors Actuators, A Phys.*, **89**, 64 (2001).